Unprecedented reduction and quick recovery of the South Indian Ocean heat content and sea level in 2014-2018

Denis L. Volkov[1,2]

Sang-Ki Lee[2], Arnold L. Gordon[3], Michael Rudko[1,2]

[1]Cooperative Institute for Marine and Atmospheric Studies, University of Miami, Miami, FL, USA

[2]NOAA Atlantic Oceanographic and Meteorological Laboratory, Miami, FL, USA

[3]Lamont-Doherty Earth Observatory, Columbia University, Palisades, NY, USA

Ocean Surface Topography Science Team meeting, October 19-23, 2020

Photo taken in the western Indian Ocean during the I07N GO-SHIP cruise in Apr-Jun 2018

1. Introduction

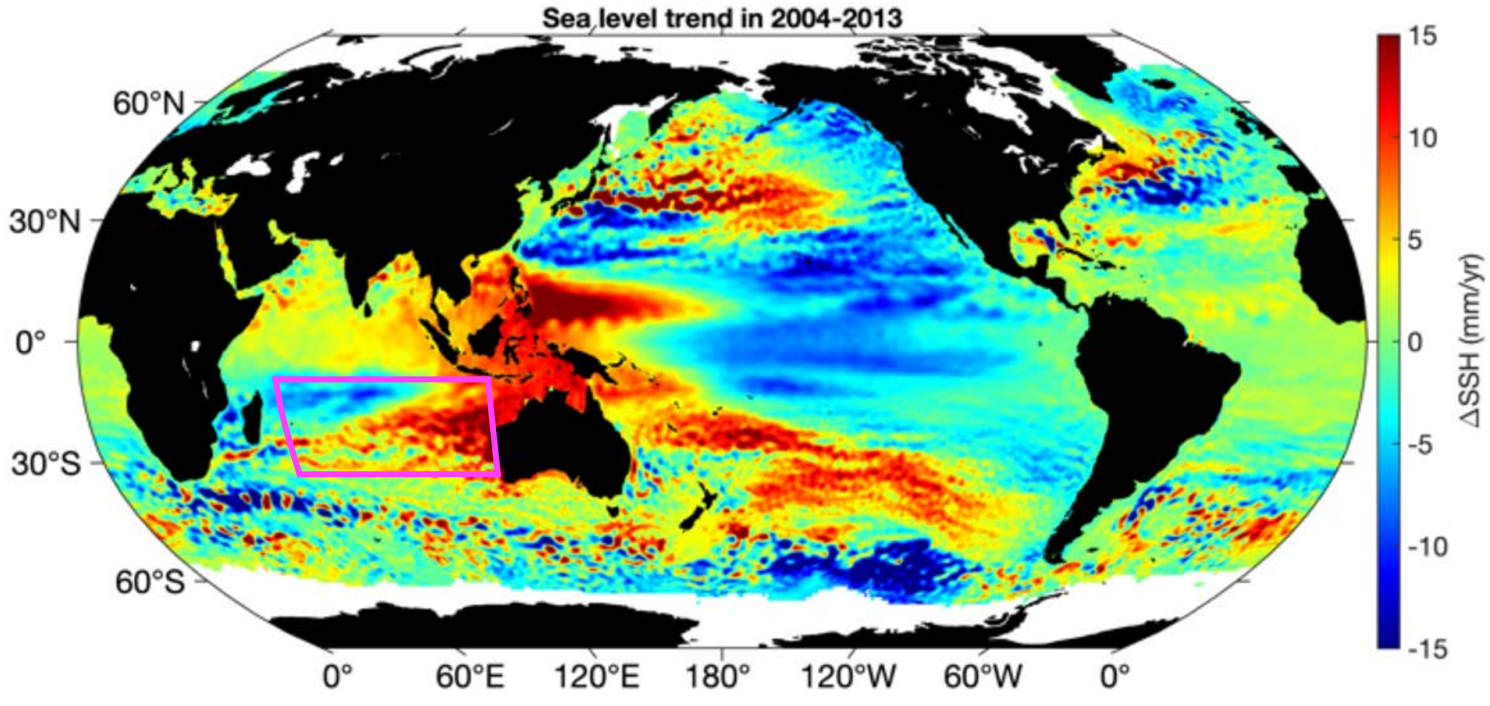

- The South Indian Ocean (SIO) has been one of the major basins for regional heat accumulation and sea level rise, in particular in 2004-2013
- The year-to-year sea level variability (black curve) in the SIO is mostly thermosteric (red curve), i.e., due to changes in heat content

- Following the onset of the very strong El Niño, the decade-long upper-ocean warming in 2004-2013 ended with an unprecedented cooling in 2014-2016, followed by a quick recovery during the weak 2017-2018 La Niña
- Interestingly, no similar cooling occurred during the strongest on record 1997-1998 El Niño event

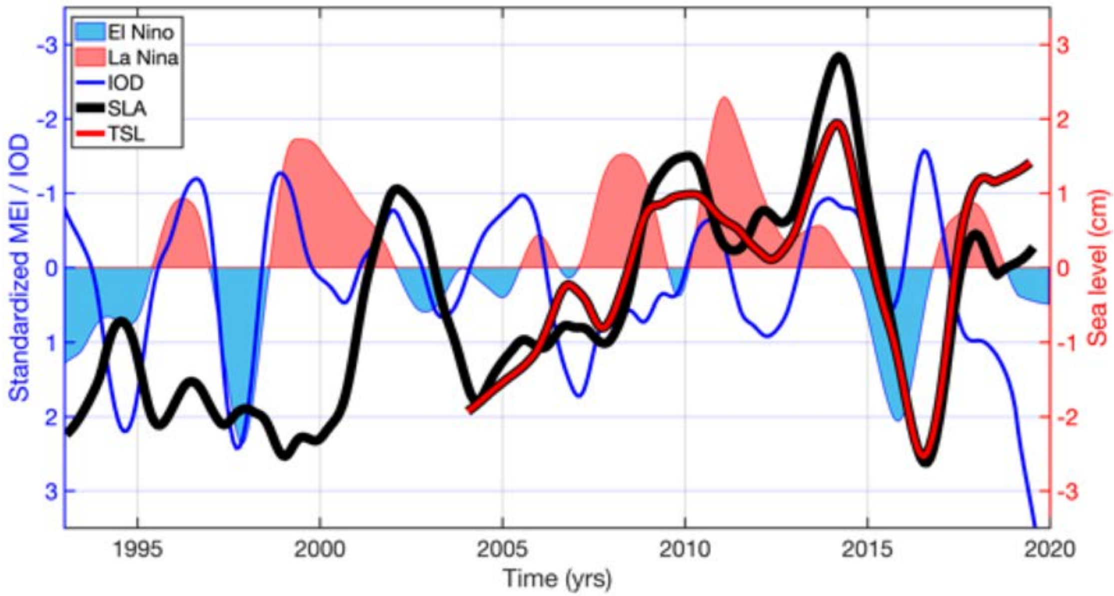

2. Objectives and Materials

Objectives:

- Investigate the mechanisms of the abrupt 2014-2016 cooling and the 2017-2019 warming in the subtropical SIO
- Characterize the difference in oceanic and atmospheric conditions during the two strongest on record El Niño events in 1997–1998 and in 2014–2016

Data used:

- Monthly satellite altimetry maps of sea level anomalies (AVISO)
- Argo gridded data (SIO, Roemmich and Gilson, 2009)
- Wind velocity and surface wind stress from ERA-Interim (Dee et al., 2011)
- Multivariate ENSO Index (MEI, Wolter and Timlin, 2011)
- The data are low-pass filtered with a cutoff period of 1 year

3. Dynamic processes affecting the South Indian Ocean heat content

The interannual-to-decadal variability of heat content and sea level in the SIO is strongly influenced by its connection with the Pacific and large-scale climatic forcing in the Indo-Pacific region: El Niño–Southern Oscillation (ENSO), Indian Ocean Dipole (IOD), and Southern Annular Mode (SAM).

The remote ENSO effect on the SIO heat content is twofold: (i) ENSO drives changes in the upper-ocean heat content in the western equatorial Pacific and, therefore, modulates advection into the SIO from the Pacific, which we term here the **"ocean tunnel"** effect; (ii) local changes in wind stress curl influencing the upper-ocean heat content in the SIO are also related to ENSO by the means of atmospheric teleconnections via the Walker Circulation, which we call here the **"atmospheric bridge"** effect. While the atmospheric bridge is a rather fast teleconnection, it takes years for the ocean tunnel signals to reach the western Indian Ocean.

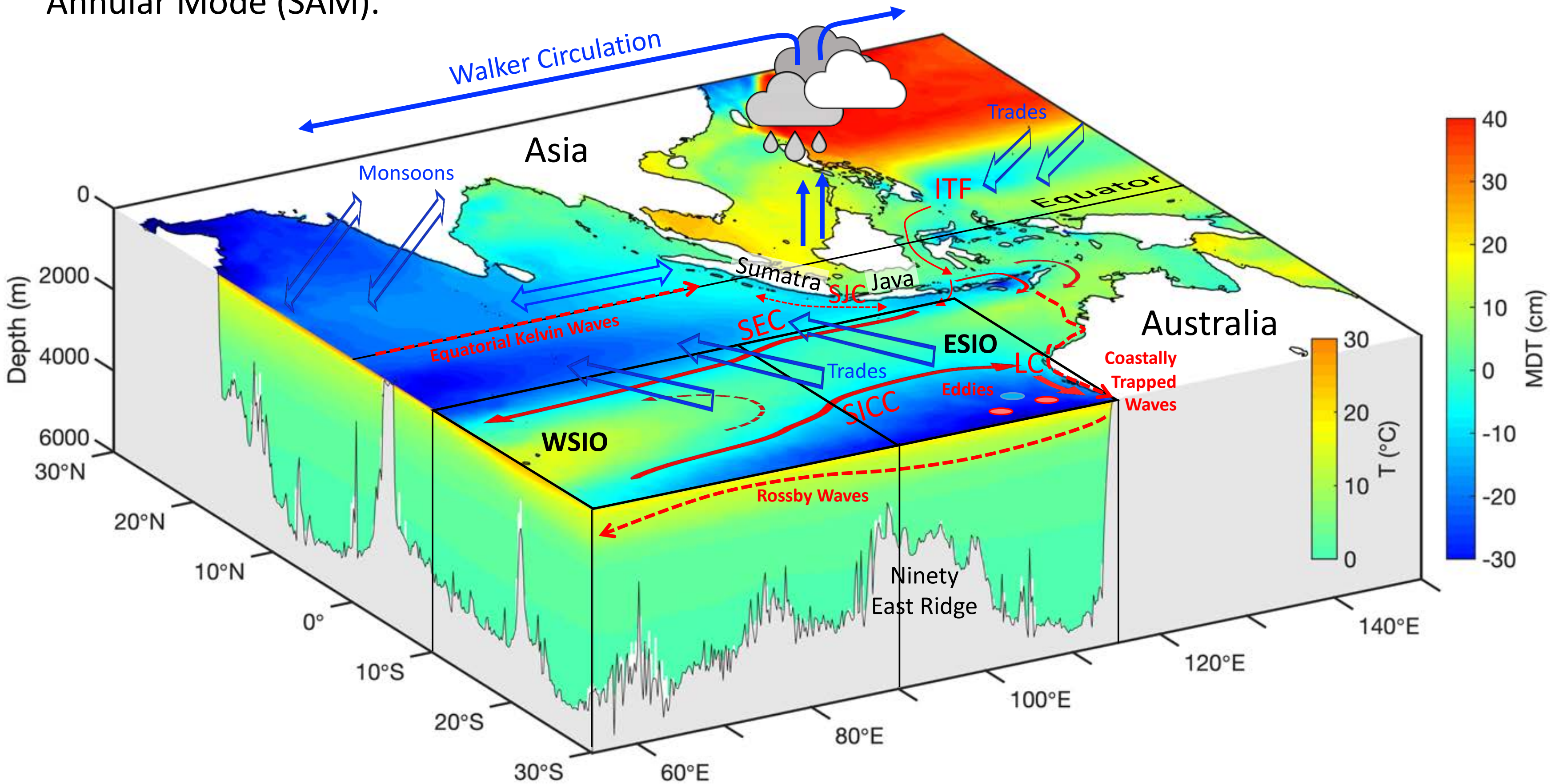

The main conduit of warm water from the Pacific to the SIO is the **Indonesian Throughflow (ITF)**, which is generally stronger/weaker during La Niña/El Niño conditions and positive/negative IOD events. Temperature anomalies entering the SIO via the ITF can also affect **coastal trapped waves** along the west Australian coast. From the eastern boundary, these signals radiate westward as **Rossby waves** and mesoscale eddies, and eventually affect sea level and heat content in the SIO interior. On seasonal-to-interannual time scales, local wind forcing, through **Ekman pumping** over the open ocean and coastal upwelling, is also able to generate Rossby waves and/or modify those emanated from the eastern boundary.

4. Spatial structure of sea level changes in 2014-2018

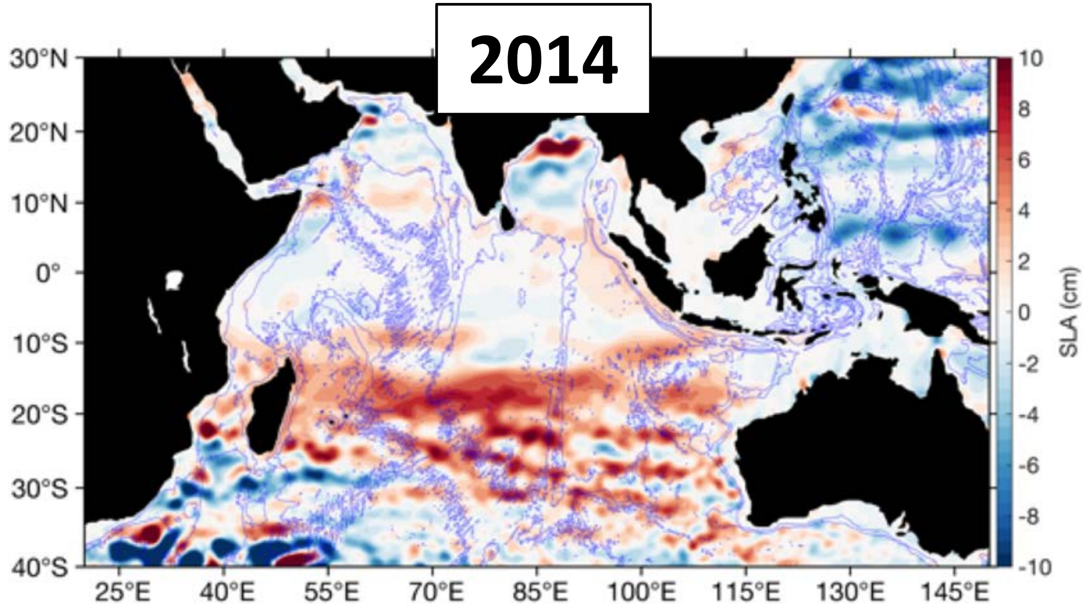

The 2014-2016 cooling (negative SLA in 2016) in the SIO was basin-wide. In contrast, the 2017-2018 warming (positive SLA in 2018) mainly occurred in the western SIO (WSIO; west of the Ninety East Ridge), while the eastern SIO (ESIO; east of the Ninety East Ridge) still exhibited low SLA remaining there since the 2014–2016 El Niño. This raises **a question** on *whether the weak La Niña in 2017–2018 and the westward propagation of temperature anomalies had any notable contribution to the heat content variability in the WSIO in 2014–2018*?

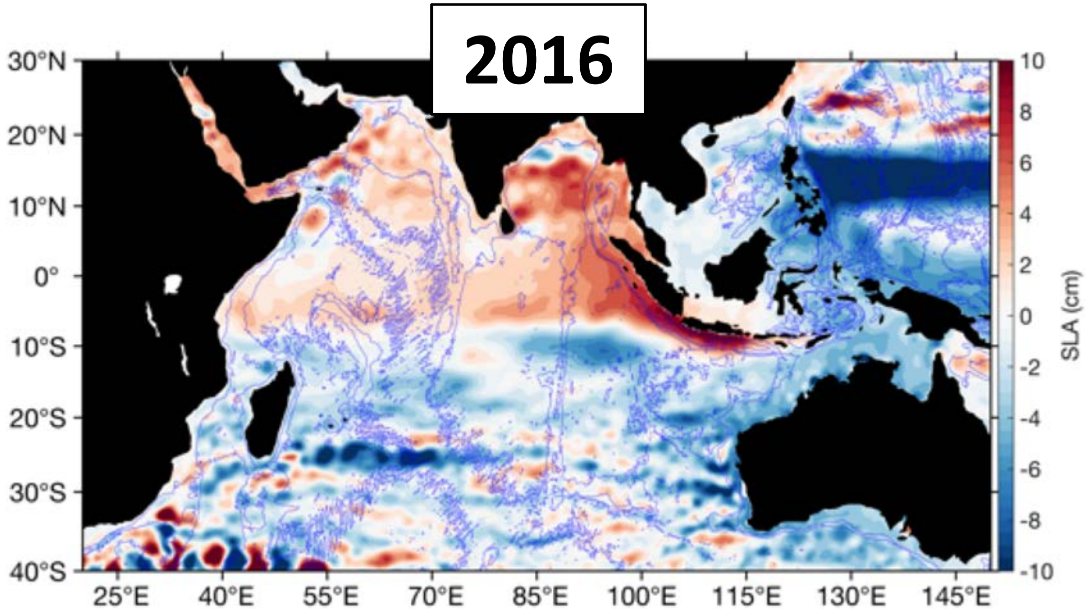

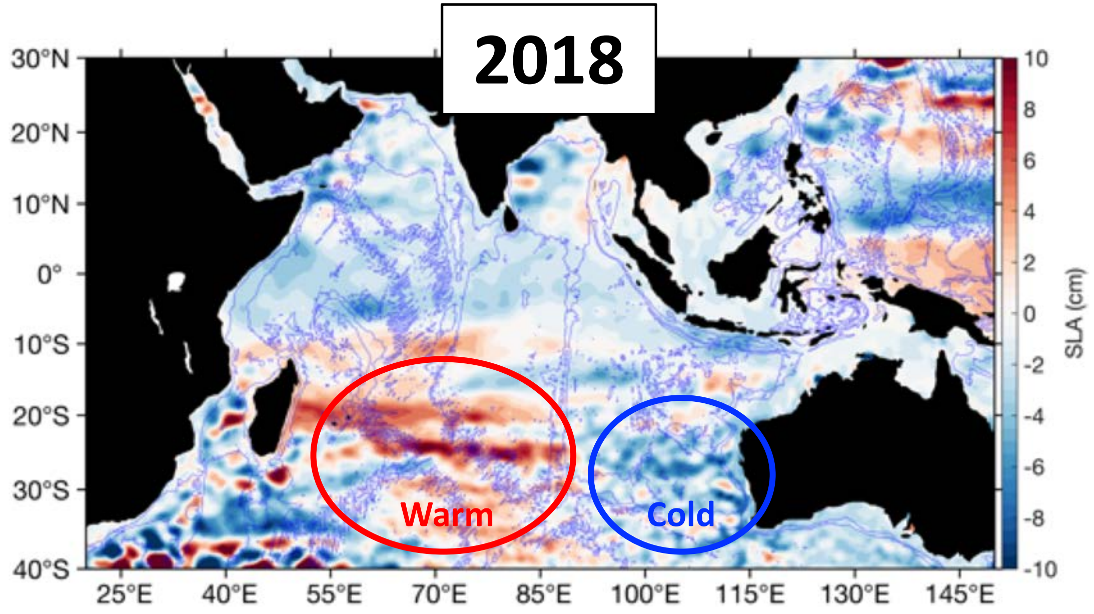

5. Westward propagation of sea level and heat content anomalies

- **Westward propagation** is the most prominent feature of the (low-pass filtered) year-to-year SLA changes

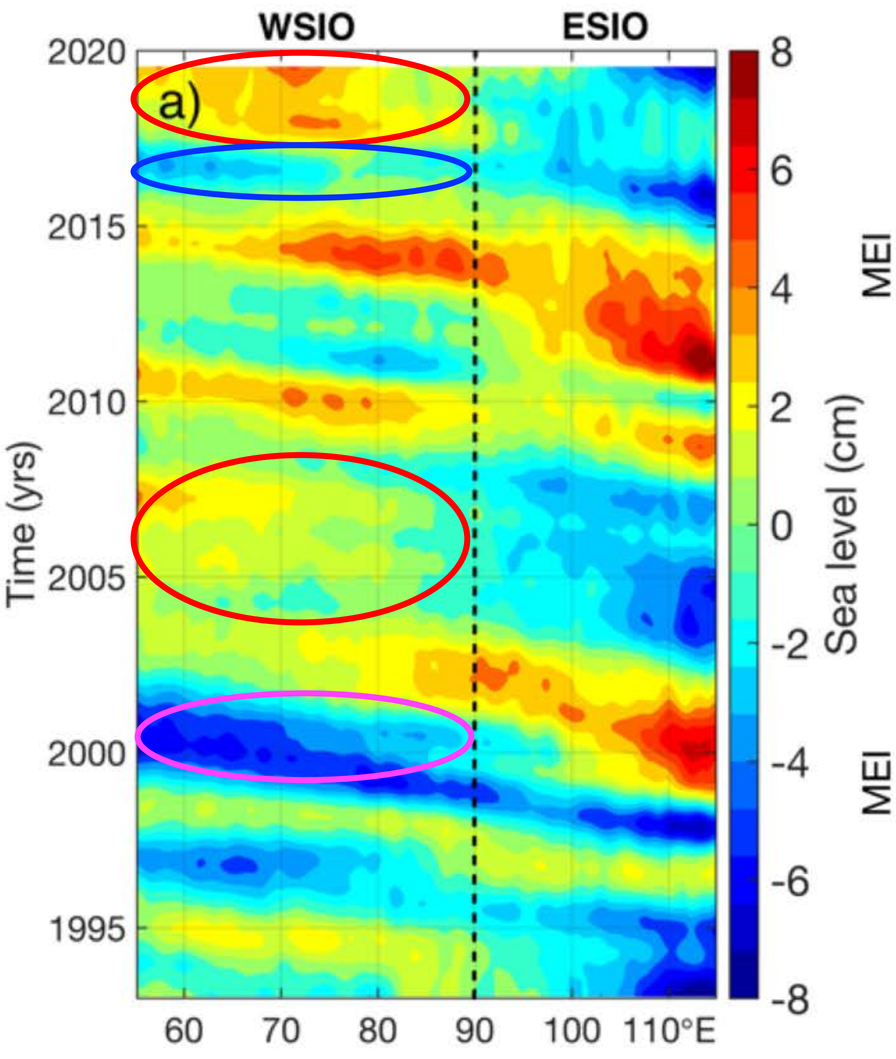

- Interannual SLA variability is mostly thermosteric (red curves), while halosteric change is smaller (green curves): **SLA is a good proxy for heat content changes**

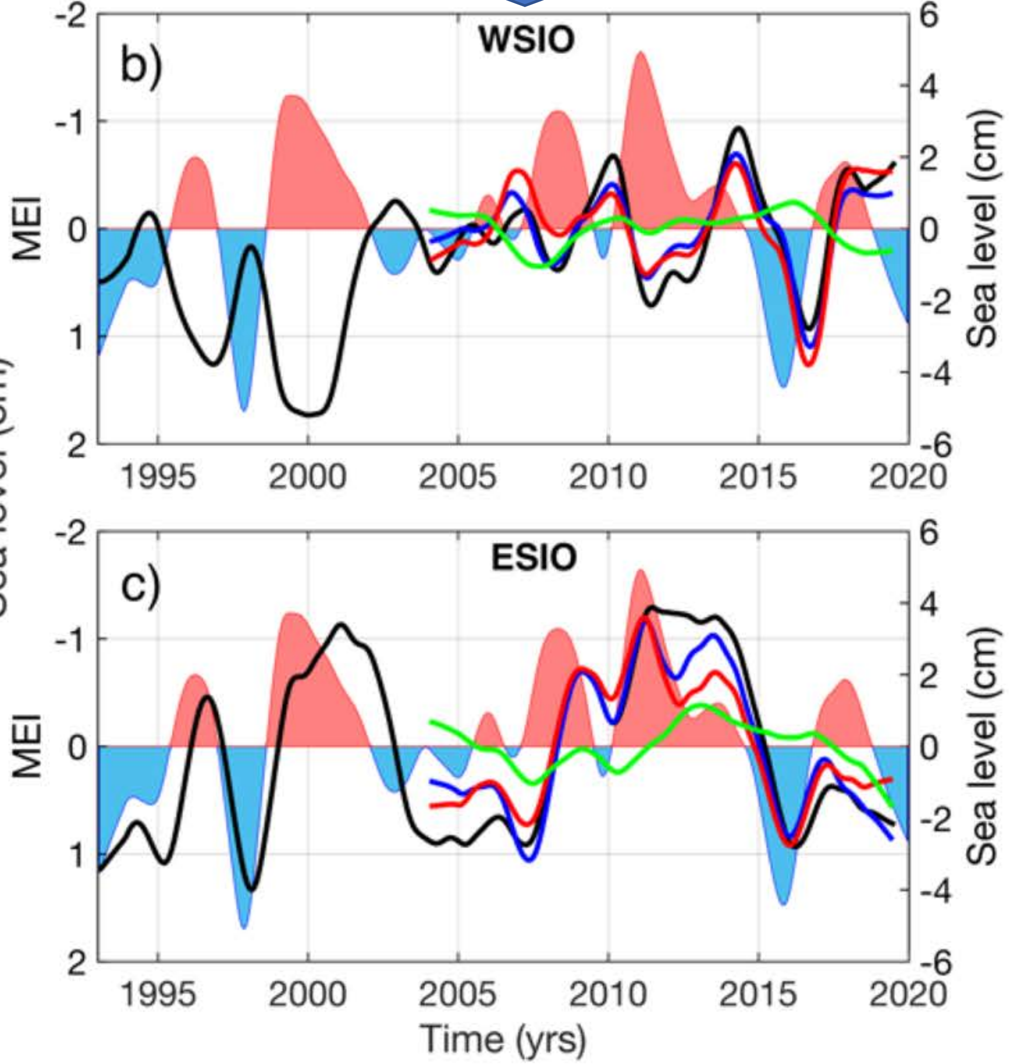

- Not all signals radiated from the eastern boundary are able to cross the entire SIO
- Westward propagation does not explain some anomalies in the WSIO (to the west of the Ninety East Ridge):
  - ✓ **Warm anomalies in 2005-2008 and in 2017-2019 (red ovals)**
  - ✓ **Cold anomaly in 2017 (blue oval)**
  - ✓ **Amplification of cold anomaly in 2000 (magenta oval)**
- Due to the “ocean tunnel” effect, SLA signals in the ESIO are well correlated with ENSO

6. Local wind forcing

The regression of wind and Ekman pumping anomalies on Multivariate ENSO Index (left) and Indian Ocean Dipole index (right)

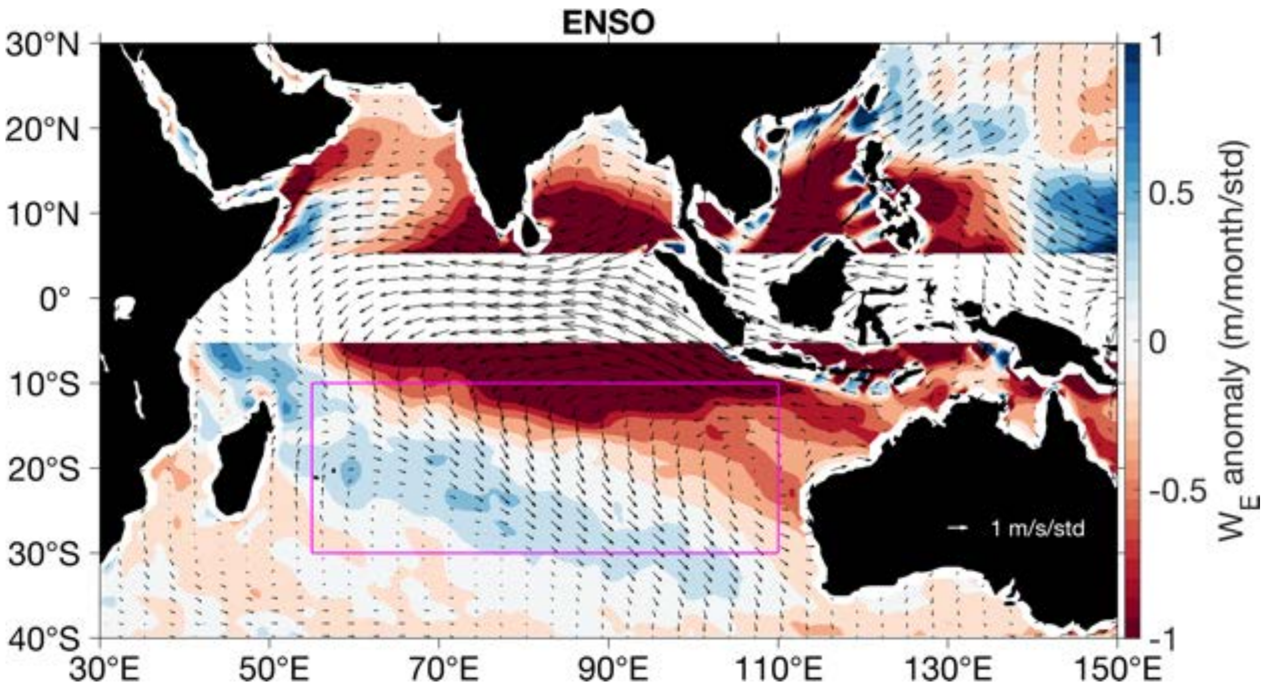

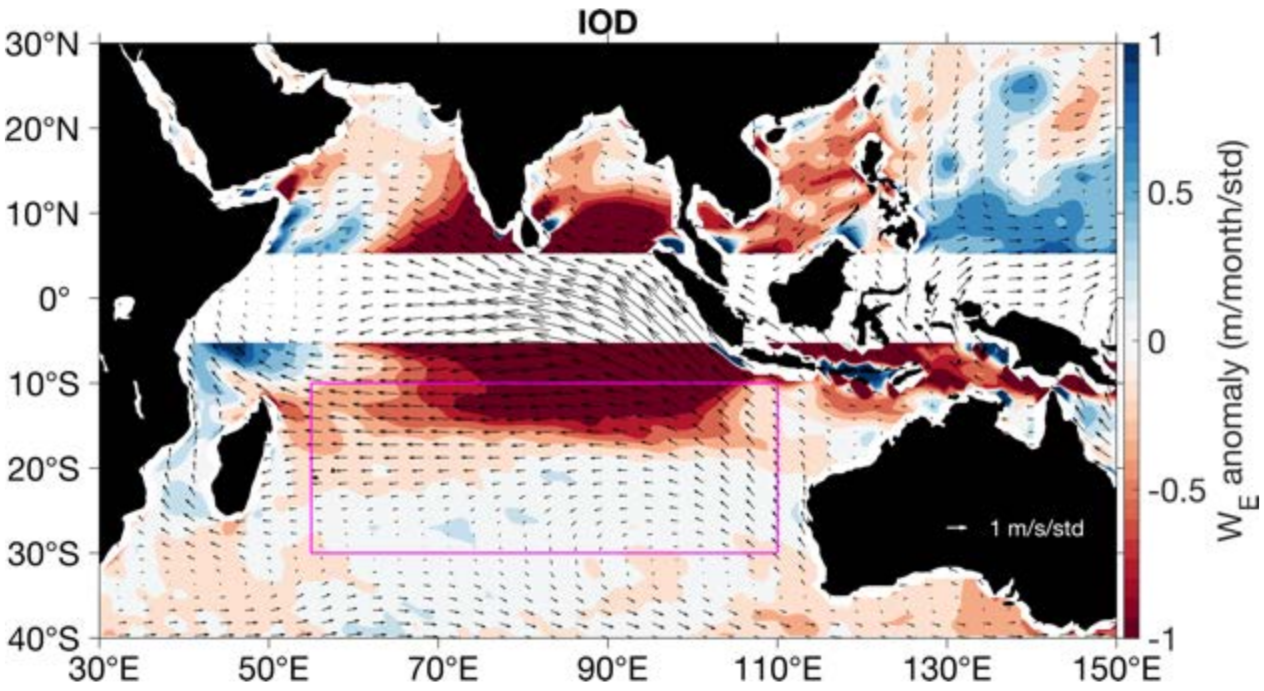

El Niño events (positive MEI) are associated with weaker trade winds in the SIO and easterly wind anomalies along the equator. This atmospheric circulation pattern favors negative Ekman pumping anomaly in the northeastern SIO and positive Ekman pumping anomaly in the southwestern SIO, leading to the upper-ocean warming (red colors) and cooling (blue colors), respectively. The opposite occurs during La Niña events (negative MEI).

Easterly equatorial wind anomalies can lead to the upper-ocean warming (red colors) between about 15°S to 15°N during a positive IOD phase and vice versa during a negative IOD phase, with a rather small response in the subtropical SIO.

6. Local wind forcing

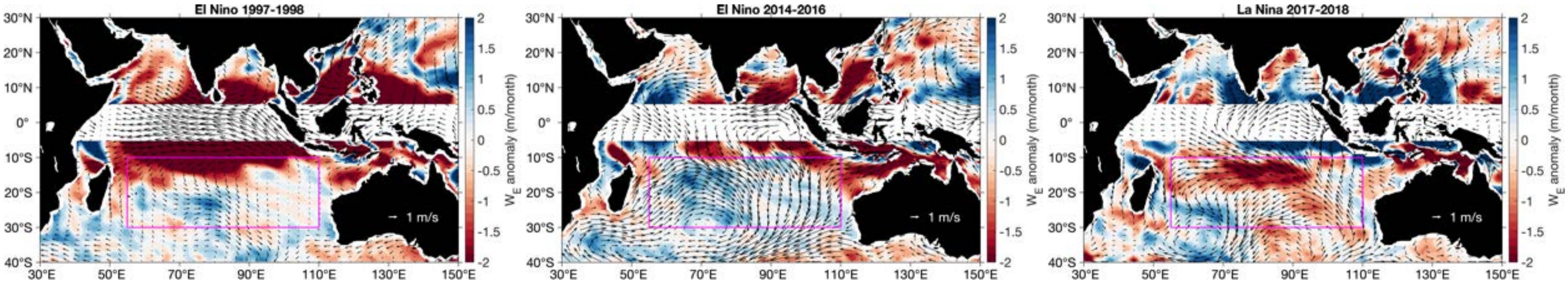

A comparison of atmospheric circulation patterns during the two strongest El Niño events in 1997–1998 and in 2014–2016 provides another explanation why the basin-wide oceanic response to the former was much weaker than that to the latter. The two main differences between these two time periods were the presence of strong easterly equatorial winds in 1997–1998, which was not observed in 2014–2016, and the presence of basin-wide cyclonic wind anomaly in 2014–2016, which was not found in 1997–1998. Strong equatorial easterlies in 1997–1998 generated downward Ekman pumping anomalies and favored the upper-ocean warming in the tropics, apparently compensating for the El Niño–generated cooling in the ESIO from the ocean tunnel effect. In contrast to the 1997–1998 El Niño, the 2014–2016 El Niño was characterized by weaker southeasterly trade winds and a cyclonic (clockwise) wind anomaly over the entire SIO. This led to Ekman divergence and associated (upward) Ekman pumping anomalies, which favored the observed reduction of the upper-ocean heat content. In 2017–2018, southeasterly trade winds strengthened, leading to downward Ekman pumping anomalies over most of the SIO.

7. Upper-ocean temperature changes

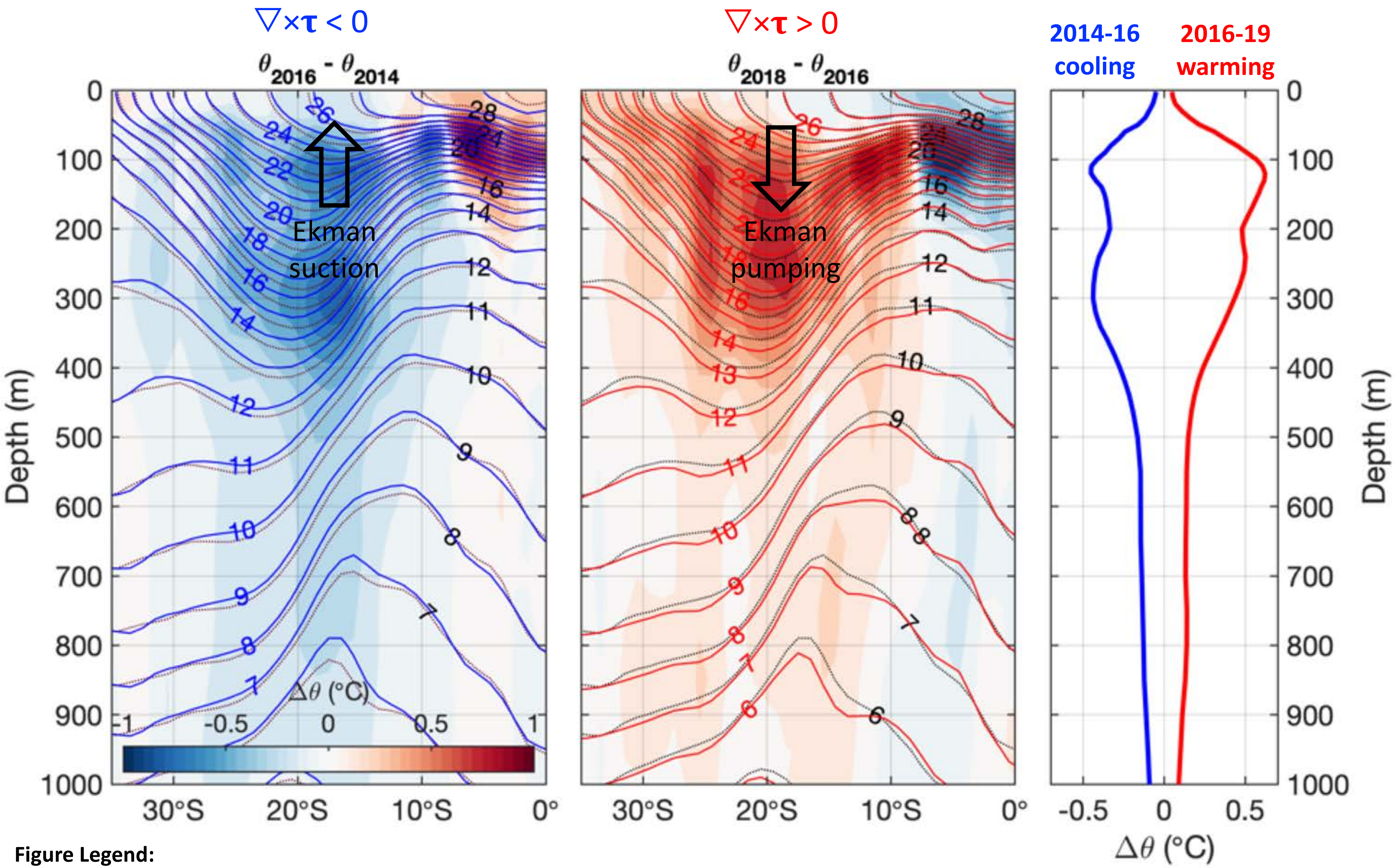

- The upper-ocean temperature changes are consistent with wind stress curl forcing
- Wind stress curl appears to affect temperature in the upper 1000 m
- The maximum temperature changes occurred between ~100-300 m (i.e. below the upper Ekman layer)

Figure Legend:

Profiles of the low-pass–filtered potential temperature, θ, averaged between 55°E and 110°E: (**left**) in 2016 (θ_{2016}; blue contour), in 2014 (θ_{2014}; black dotted contour), and their difference, $\theta_{2016} - \theta_{2014}$ (color); (**middle**) in 2018 (θ_{2018}; red contour), in 2016 (θ_{2016}; black dotted contour), and their difference, $\theta_{2018} - \theta_{2016}$ (color); and (**right**) $\theta_{2016} - \theta_{2014}$ (blue line) and $\theta_{2018} - \theta_{2016}$ (red line) differences averaged between 55°E to 110°E and 10°S to 30°S.

8. Model for sea level variability

In the SIO, the large-scale interannual sea level variations can be largely explained by the westward propagating Rossby waves that either radiate from the eastern boundary being strongly linked to signals coming from the Pacific or they are generated by local wind forcing.

Rossby Waves in the SIO

Radiate from the eastern boundary
(linked to signals coming from the Pacific)

Generated by local wind forcing

- **Long-wave linear vorticity equation for the baroclinic component of SLA:**

$$\frac{\partial \eta}{\partial t} = c_R \frac{\partial \eta}{\partial x} - \frac{g' \nabla \times \boldsymbol{\tau}}{\rho_0 g f} - \varepsilon \eta$$

η – sea level anomaly; c_R - zonal phase speed of long baroclinic Rossby waves;
g' – reduced gravity; $\boldsymbol{\tau}$ – wind stress; ε – frictional damping coefficient

- **Solution in the longitude-time (x-t) plane** (Qui, 2002; Zhuang et al., 2018)**:**

$$\eta(x,t) = \boxed{\eta\left(x_e, t - \frac{x - x_e}{c_R}\right) e^{-\varepsilon\left(\frac{x - x_e}{c_R}\right)}} - \boxed{\frac{g'}{\rho_0 g f c_R} \int_{x_e}^{x} \nabla \times \boldsymbol{\tau}\left(x', t - \frac{x - x'}{c_R}\right) e^{-\varepsilon\left(\frac{x - x'}{c_R}\right)} dx'}$$

Signal radiated from the eastern boundary

Signal generated by local wind forcing

9. Local (wind stress) vs remote (eastern boundary) forcing: observations vs model

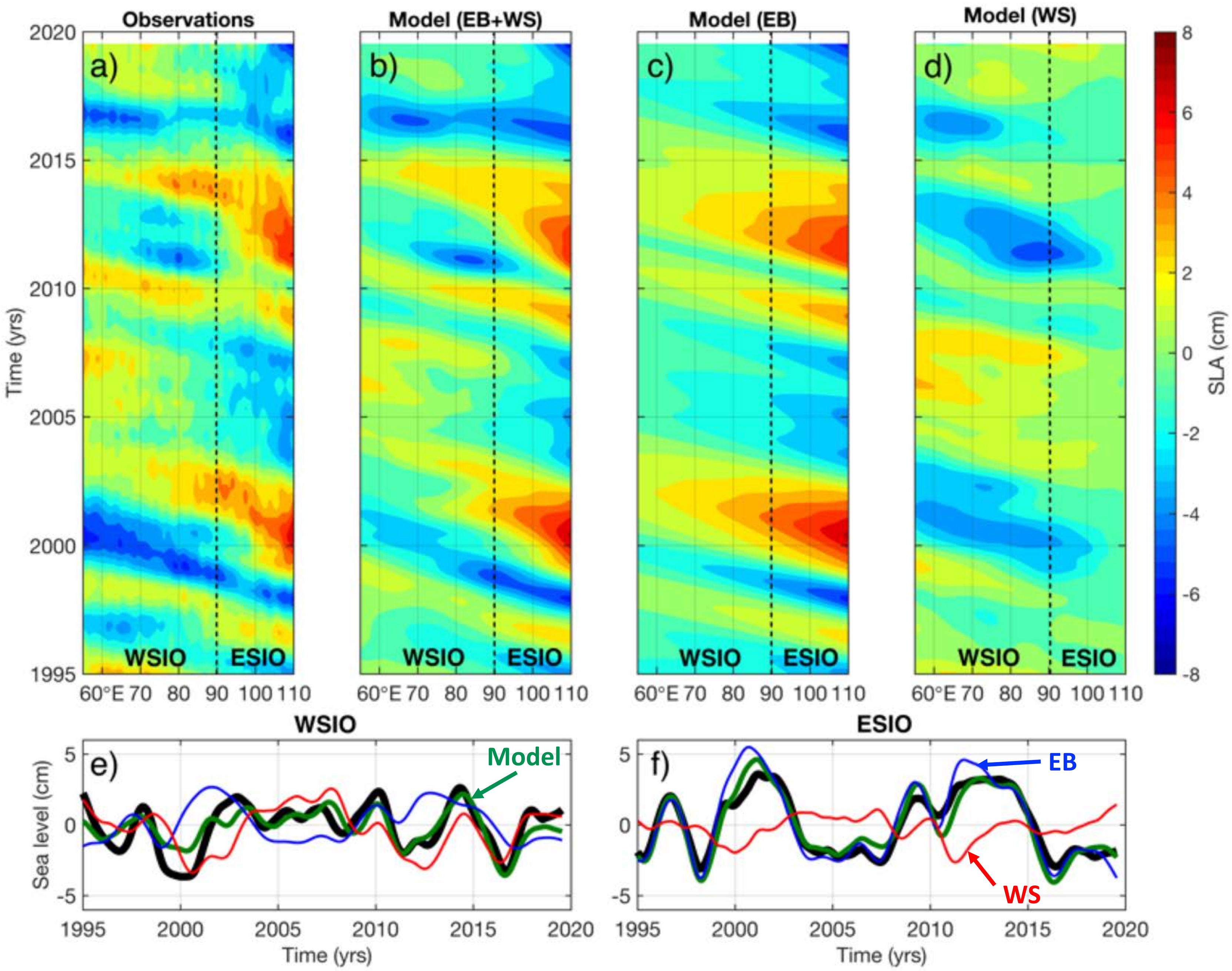

- The eastern boundary (EB) and wind stress curl (WS) forcing terms together simulate the observed SLA rather well
- Both forcing terms have similar magnitudes
- The local wind stress curl ("atmospheric bridge" effect) dominates SLA variability in the WSIO, while the eastern boundary forcing ("ocean tunnel" effect) is dominant in the ESIO
- The 2014-2016 basin-wide cooling occurred due to a rather unusual combination of the atmospheric bridge and ocean tunnel effects, amplifying each other
- Local wind stress curl appears to be the only reason for the observed recovery of the SIO heat content in 2017-2019

10. Summary and Conclusions

- The interannual variability of the upper-ocean heat content and sea level in the SIO is tightly linked to remote processes originating in the Pacific, to local wind forcing, and to mesoscale ocean dynamics (westward propagation)

- The interannual variability of sea level and heat content in 1993-2019 was dominated by the local wind forcing in the WSIO and by the eastern boundary (remote) forcing in the ESIO

- The unprecedented basin-wide decrease of sea level and heat content in 2014–2016 occurred because of a rather unusual condition, during which the atmospheric bridge and ocean tunnel effects worked constructively, amplifying the impact of each other.

- The subsequent recovery in 2017–2018 was mainly driven by an anticyclonic wind anomaly formed over the SIO during the weak La Niña via the atmospheric bridge effect.

- Compared with the 2014–2016 El Niño, there was no similar wind-driven basin-wide cooling in the SIO during the strongest on record 1997–1998 El Niño. Additionally, when the El Niño–generated negative SLA was present in the ESIO in 1997–1998, the positive SLA generated during the 1995–1996 La Niña reached the WSIO, thus resulting in a small net change of SLA in the subtropical SIO during 1996–1998.

For more details, please refer to the following publication:

Volkov D.L. , S.-K. Lee, A.L. Gordon, M. Rudko (2020), Unprecedented reduction and quick recovery of the South Indian Ocean heat content and sea level in 2014-2018, *Science Advances*, 6(36), eabc1151, https://doi.org/10.1126/sciadv.abc1151.

Acknowledgements: This work was supported by the NASA Ocean Surface Topography Science Team program (via the grant NNX17AH59G) and partially by the NOAA Atlantic Oceanographic and Meteorological Laboratory. The research was carried out, in part, under the auspices of the Cooperative Institute of Marine and Atmospheric Studies (CIMAS), a Cooperative Institute of the University of Miami and NOAA (cooperative agreement NA10OAR4320143).